A Physicochemical Approach for Predicting the Effectiveness of Peptide-Based Gene Delivery Systems for Use in Plasmid-Based Gene Therapy

John G. Duguid,* Cynthia Li,* Mei Shi,* Mark J. Logan,* Hector Alila,* Alain Rolland,* Eric Tomlinson,* James T. Sparrow,# and Louis C. Smith#

*GeneMedicine, The Woodlands, Texas 77381-4248, and #Department of Medicine, Baylor College of Medicine, Houston, Texas 77030-2707 USA

ABSTRACT Novel synthetic peptides, based on carrier peptide analogs ($YKAK_nWK$) and an amphipathic peptide (GLFEALLELLESLWELLLEA), have been formulated with DNA plasmids to create peptide-based gene delivery systems. The carrier peptides are used to condense plasmids into nanoparticles with a hydrodynamic diameter (D_H) ranging from 40 to 200 nm, which are sterically stable for over 100 h. Size and morphology of the carrier peptide/plasmid complex have been determined by photon correlation spectroscopy (PCS) and transmission electron microscopy (TEM), respectively. The amphipathic peptide is used as a pH-sensitive lytic agent to facilitate release of the plasmid from endosomes after endocytosis of the peptide/plasmid complex. Hemolysis assays have shown that the amphipathic peptide destabilizes lipid bilayers at low pH, mimicking the properties of viral fusogenic peptides. However, circular dichroism studies show that unlike the viral fusion peptides, this amphipathic peptide loses some of its α-helical structure at low pH in the presence of liposomes. The peptide-based gene delivery systems were tested for transfection efficiency in a variety of cell lines, including 14-day C_2C_{12} mouse myotubes, using gene expression systems containing the β-galactosidase reporter gene. Transfection data demonstrate a correlation between in vitro transfection efficiency and the combination of several physical properties of the peptide/plasmid complexes, including 1) DNA dose, 2) the zeta potential of the particle, 3) the requirement of both lytic and carrier peptides, and 4) the number of lysine residues associated with the carrier peptide. Transfection data on 14-day C_2C_{12} myotubes utilizing the therapeutic human growth hormone gene formulated in an optimal peptide gene delivery system show an increase in gene expression over time, with a maximum in protein levels at 96 h (~18 ng/ml).

INTRODUCTION

Among several methods of gene transfer, including cell-based and viral-mediated approaches, nonviral gene delivery is becoming a major focus of research in the field of gene therapy (Ledley, 1994, 1995; Rolland, 1996, 1997; Rolland and Tomlinson, 1996; Tomlinson and Rolland, 1996). This increased interest in nonviral gene therapy can be attributed to promising results both, in vitro and in vivo, in delivering genes using proteins (Cotten et al., 1990, 1993; Plank et al., 1992; Trubetskoy et al., 1992; Wagner et al., 1990, 1991, 1992; Wang and Huang, 1989; Wu and Wu, 1987, 1988a,b), high-molecular-weight polypeptides (Cotten et al., 1990; Erbacher et al., 1995; Midoux et al., 1993; Monsigny et al., 1994; Wagner et al., 1990, 1991), cationic lipids and liposomes (Dowty and Wolff, 1994; Felgner et al., 1987; Legendre and Szoka, 1992; Trubetskoy et al., 1992; Wang and Huang, 1989), novel synthetic polymers (Boussif et al., 1995; Haensler and Szoka, 1993; Kabanov and Kabanov, 1995), or combinations thereof (Plank et al., 1994; Remy et al., 1995; Trubetskoy et al., 1992; Wagner et al., 1991; Zhou et al., 1991). The utilization of many of these delivery systems stems from their ability to interact with a plasmid and self-assemble into compact particles (Bloomfield et al., 1992; Chattoraj et al., 1978; Evdokimov et al., 1973, 1976; Ghirlando et al., 1992; Gosule and Schellman, 1976; Haynes et al., 1970; Hirschman et al., 1967; Laemmli, 1975; Lerman, 1971; Olins et al., 1967; Shapiro et al., 1969; Widom and Baldwin, 1980, 1983; Wilson and Bloomfield, 1979). Some polymers have been conjugated to targeting ligands for cell-specific gene delivery, resulting in enhanced gene transfer efficiency via the route of receptor-mediated endocytosis (Cotten et al., 1993; Erbacher et al., 1995; Gottschalk et al., 1993; Midoux et al., 1993; Monsigny et al., 1994; Plank et al., 1992; Wagner et al., 1990, 1991; Wu and Wu, 1987, 1988a,b). Endosomolytic agents are regularly introduced into the gene delivery system to prevent lysosomal plasmid degradation and subsequently improve the translocation of a plasmid to the nucleus of a target cell (Fattal et al., 1994; Gottschalk et al., 1996; Haensler and Szoka, 1993; Legendre and Szoka, 1993; Parente et al., 1990a,b; Plank et al., 1994; Subbarao et al., 1987; Wagner et al., 1992).

Most of the polypeptide gene delivery systems present a heterogeneous, high-molecular-weight component. Such macromolecules, which are generally highly charged, have a propensity to elicit an immune response and are often cytotoxic. In addition, it has been suggested that biologically active regions of many proteins consist of residues that are only 10–20 amino acids in length (Gottschalk et al., 1996). The use of high-molecular-weight polypeptides may

Received for publication 15 October 1996 and in final form 27 February 1998.

Address reprint requests to Dr. John G. Duguid, Gene Delivery Department, GeneMedicine, 8301 New Trails Drive, The Woodlands, TX 77381-4248. Tel.: 281-364-1150; Fax: 281-364-0858; E-mail: biojohn@aol.com.

Dr. Li's present address is Amgen, 1840 Dehavilland Dr., Thousand Oaks, CA 91320-1789.

0006-3495/98/06/2802/13 $2.00

not be necessary, because it has been shown that low-molecular-weight counterions with more than two positive charges are capable of inducing DNA condensation into compact structures (Bloomfield et al., 1992; Chattoraj et al., 1978; Gosule and Schellman, 1976; Widom and Baldwin, 1980, 1983; Wilson and Bloomfield, 1979). In one instance it has been shown that a divalent transition-metal cation is capable of condensing DNA (Ma and Bloomfield, 1994). Whereas the packaging of DNA into condensed particles has been studied extensively (Bloomfield, 1992; Bloomfield et al., 1980; Duguid and Bloomfield, 1996; Eickbush and Moudrianakis, 1978; Hud, 1995; Hud et al., 1995; Li et al., 1991; Manning, 1980, 1981, 1985; Post and Zimm, 1979, 1982a,b; Richards et al., 1973), only recently have attempts been made to identify the properties of the condensed plasmid that influence transfection efficiency (Bloomfield, 1996; Tang and Szoka, 1997). Several such attempts have focused primarily on lipid and liposome-based condensed systems (Gao and Huang, 1995; Gershon et al., 1993; Gustafsson et al., 1995; Labat-Moleur et al., 1996; Rädler et al., 1997; Reimer et al., 1995; Smith et al., 1993; Sternberg et al., 1994).

In this publication we describe the correlation between some of the physical characteristics of a peptide/plasmid gene delivery system and its ability to transfect cells in vitro. Short oligolysine peptides (GM208-GM240) with the sequence YKA$(K)_n$WK, where $n = 4-8$, 12, and 40, have been synthesized (Gottschalk et al., 1996). The effects of their interactions with plasmids on particle size has been analyzed as a function of peptide/DNA charge ratio, number of lysine residues, DNA concentration, and time. An amphipathic, pH-sensitive peptide (GM225.1) with the sequence GLFEALLELLESLWELLLEA has been incorporated into the peptide/plasmid complex to effect intracellular trafficking of the peptide-gene delivery system (Gottschalk et al., 1996). The endosomolytic peptide GM225.1 is shown to be membrane active at pH 5.0 but not at pH 7.4. This pH-dependent lytic activity prevents damage to the plasma membrane, while inducing modification of the endosomal membrane, thus enabling plasmids to be released from endosomes into the cytoplasm.

The peptide-based gene delivery systems were tested for transfection efficiency in a variety of cell lines, including RAW264.7 mouse macrophages, HIG-82 rabbit synoviocytes, and C_2C_{12} mouse myotubes, by use of a gene expression system containing the β-galactosidase reporter gene. The necessity of both carrier and lytic peptide for effective gene transfer was assessed. Physicochemical properties of the delivery systems were simultaneously analyzed (e.g., pH, particle size, and zeta potential). Transfection efficiency in 14-day C_2C_{12} myotubes was also tested as a function of the number of lysine residues in the carrier peptide. The experimental data were analyzed as correlation plots and revealed a relationship between transfection efficiency and parameters, including the presence of lytic and carrier peptides, the number of lysine residues in the carrier molecule, DNA dose, and zeta potential of the complex.

As part of the development of a novel gene delivery system for the transfer of human growth hormone (hGH) gene to muscle cells, a prototype peptide-based gene delivery system was tested in vitro. Transfection efficiency of a peptide delivery system was assessed in 14-day myotubes by quantitation of the levels of hGH secreted in the culture medium.

MATERIALS AND METHODS

Preparation of the gene expression systems

Both the reporter gene expression system (CMV-β-gal), containing the β-galactosidase reporter gene driven by the cytomegalovirus (CMV) promoter, and the therapeutic gene expression system (sk-hGH), containing the human growth hormone gene (hGH) driven by the chicken skeletal-α actin (sk) promoter, were prepared, purified, and quality controlled at GeneMedicine.

Peptide synthesis and purification

The carrier peptides GM204 ($YKAK_4WK$), GM205 ($YKAK_5WK$), GM206 ($YKAK_6WK$), GM207 ($YKAK_7WK$), GM208 ($YKAK_8WK$), GM212 ($YKAK_{12}WK$), and GM240 ($YKAK_{40}WK$), and the amphipathic peptide GM225.1 (GLFEALLELLESLWELLLEA) were synthesized by the solid phase method developed by Merrifield (Barany and Merrifield, 1980), using fast HBTU/HOBT (HBTV, 2-(1*H*-benzotriazol-l-yl)-1,1,3,3-tetramethyluroniumhexafluorophosphate; HOBT, *N*-hydroxybenzotriazole) coupling (Reid and Simpson, 1992) as described previously (Gottschalk et al., 1996).

Both carrier and endosomolytic peptides were purified by reversed-phase high-performance liquid chromatography (HPLC) (Hancock and Sparrow, 1981, 1984). Carrier peptides were initially diluted in 1% trifluoroacetate (TFA) and loaded on a 2.5 × 25 cm Vydac C18 column equilibrated in 0.1% TFA. The peptides were eluted using a linear gradient from 0.1% TFA to 0.1% TFA with 10% 2-propanol at a flow rate of 20 ml/min. After elution, the purified peptides were collected, lyophilized, and redissolved in MilliQ water.

GM225.1 was diluted in 0.1 M ammonium phosphate in 6 M guanidine HCl (pH 6.7) and loaded onto a 2.5 × 25 cm Vydac C4 column equilibrated in 0.01 M ammonium phosphate. The peptides were eluted using a linear gradient from 0.01 M ammonium phosphate (pH 6.7) and 30% 2-propanol to 0.01 M ammonium phosphate and 50% 2-propanol at a flow rate of 20 ml/min. After elution, peptide fractions were pooled, adjusted to pH 8.0 with ammonium hydroxide, and desalted on a BioGel P-2 column equilibrated in 0.1 M ammonium bicarbonate. The desalted peptide was then lyophilized and redissolved in water. Dilute ammonium hydroxide was added to maintain a pH of 7.5 to completely dissolve the peptide.

Peptide purity was evaluated by the following methods: 1) analytical HPLC: for GM225.1, a linear gradient from 0% to 50% 2-propanol in 0.01 M ammonium phosphate at pH 6.8; for GM208, a linear gradient from 0% to 10% 2-propanol in 0.1% TFA; 2) fast atom bombardment or electrospray mass spectrometry; 3) amino acid analysis to verify composition; 4) automatic amino acid sequencing; and 5) capillary electrophoresis.

Physicochemical characterization of peptide-based gene delivery systems

Preparation of the peptide-based gene delivery system

Before the preparation of the peptide/plasmid complexes, the pH values of all carrier and amphipathic peptides were measured. Titrations were performed on peptide solutions in which there was a deviation greater than pH 7.0 ± 1.0. Acetic acid was used to titrate basic solutions, and ammonium hydroxide was used for acidic solution. The peptide solutions were titrated

within the desired range near pH 7.0. The gene expression systems were within the pH range 6.8–7.5. Plasmid samples were prepared in water or 0.5 mM HEPES at predetermined volumes, each in culture tubes (14-956-3D; Fisher Scientific) at the appropriate DNA concentration. The carrier peptide was added to the plasmids under constant vortexing. Typical volume ratios of carrier peptide added to DNA solution were in the range of 0.017–0.11. These samples were allowed to stand for 30 min to ensure complete complexation between the plasmid and peptide carrier. After 30 min, the amphipathic peptide (GM225.1) was added to the carrier peptide/plasmid colloidal suspension under vortexing. Volume ratios of amphipathic peptide solution/(carrier peptide plus plasmid suspension) were in the range of 0.007–0.022. No effect of volume ratios on hydrodynamic diameter or transfection efficiency was observed under these experimental conditions. All peptide/plasmid complexes were characterized for their solution pH, hydrodynamic diameter, and zeta potential. pH values were measured with a Ross combination electrode (no. 8103; Orion) and a pH meter (no. 720A; Orion).

Photon correlation spectroscopy measurements

Particle sizing measurements were conducted on each peptide-based gene delivery system to ensure that the complexes were self-assembled into compact particles. Particle size was subsequently used to determine whether cell transfection was influenced by this parameter. The particle size of the complex was determined by photon correlation spectroscopy, which computes the autocorrelation function of the intensity of light scattered by the peptide/plasmid complexes. Light scattering data were collected at a 90° angle for a period of 2 min for all formulations, using a Coulter submicron particle analyzer (model N4MD; Coulter Electronics, Hialeah, FL). Unimodal analysis was performed on each data set; here the autocorrelation function was treated as a single decaying exponential with a decay constant that is directly proportional to the diffusion coefficient (D_{trans}) of the complex. Particle size of the complex was determined from the Stokes-Einstein relation

$$D_{trans} = k_B T/3\pi\eta D_H \quad (1)$$

where k_B is Boltzmann's constant, T is the sample temperature, η is the solution viscosity, and D_H is the hydrodynamic diameter of the complex.

Transmission electron microscopy

The preparation and visualization of peptide/plasmid complexes utilized for transmission electron microscopy (TEM) studies were performed as described by Ma (1992). Briefly, carbon-coated 200-mesh copper grids (Ted Pella, Redding, CA) were glow discharged for ~90 s to render them hydrophilic. One drop of the complex of the colloidal suspension was deposited on the grids. Each grid was then stained with a drop of 1% uranyl acetate solution (Ted Pella), and excess stain was removed after 30 s. The grid was then allowed to dry for at least 20 min before TEM examination. Electron micrographs were obtained at magnifications ranging from 28,000× to 55,000× on a JEOL microscope operating at 60 kV. Particle sizes of the complexes were determined by comparing their outer diameters with grid markings.

Electrophoretic light scattering measurements

Electrophoretic light scattering (ELS) measurements enable the determination of the zeta potential (ζ) of a particle, which is proportional to its surface charge density. The zeta potential is defined as the electrical potential between the shear plane surrounding the particle and the bulk solution. ELS studies were performed on the peptide-based gene delivery system to determine whether ζ of these particles influenced cell transfection. The ζ of the complex was determined by electrophoretic light scattering with a Coulter DELSA 440 (Coulter Electronics). In the electrophoretic mobility cell, the complex was subjected to an alternating electric field in constant current mode with a magnitude no greater than 0.2 mA at 25°C. Data collection was performed periodically at two different currents to ensure that the measured zeta potentials were independent of the choice of current. The light scattering intensity was collected at 8.6°, 17.1°, 25.6°, and 34.2° angles over a minimum period of 30 s at a frequency of 500 Hz. Doppler shifts (ν) were calculated as a function of the time dependence of scattered light intensity from the moving particle in the presence of the alternating electric field. The relationship between the Doppler shift of scattered light and electrophoretic mobility (U) of the mobile complex was determined from the equation

$$U = 2\pi\nu/EK\cos\alpha \quad (2)$$

where E is the applied electric field, K is the magnitude of the scattering vector, and α is the angle between the scattering vector and the direction of migration of the complex. The ζ of the particle was determined from the equation

$$\zeta = 4\pi\eta U/\epsilon \quad (3)$$

where ϵ is the dielectric constant of the solution.

Hemolysis assay for determination of lytic peptide activity

The assay used to determine hemolytic activity was modified from the procedure of Gagne et al. (1994). Fresh blood was obtained from rats and preserved in 0.38% sodium citrate to prevent clotting. Red blood cells (RBCs) were obtained from whole blood by centrifugation in a clinical centrifuge at 2500 rpm for 10 min. Upon removal of the supernatant, the RBCs were washed with an equal volume of 1× phosphate-buffered saline (PBS) (0.144 g/liter KH_2PO_4, 9.0 g/liter NaCl, 0.726 g/liter $NaH_2PO_4{\cdot}7H_2O$). Appropriate dilutions of RBCs were made using 1× PBS before placing 15-μl aliquots between the coverslip and hemocytometer. RBCs were counted in the four corner and central squares in the two complementary hemocytometer chambers. An average RBC count per square was obtained and used to determine the number of cells per unit volume.

For the hemolysis assay, stock solutions of 2% Triton X-100 and GM225.1 were prepared separately in hemolysis buffer (150 mM NaCl, 20 mM Na citrate) at pH 5.0 and pH 7.4. In each well of a 96-well microtiter plate, 100 μl of a stock solution was diluted with 100 μl of hemolysis buffer at the same pH. Serial dilutions were performed on the solutions of GM225.1 to investigate concentration effects on hemolytic activity. RBCs were diluted to a final cell density of 1×10^8 cells/ml at the appropriate pH, from which 100-μl aliquots were added to each well and allowed to incubate at 37°C for 0, 30, 60, 120, and 180 min. After incubation, the absorbance at 540 nm (A_{540}) was measured for each sample with the EL 340 Microplate Reader (Bio-Tek Instruments, Winooski, VT). The lytic activity was calculated as the A_{540} of the RBCs in the presence of peptide, normalized between their A_{540} in the presence of Triton X-100 (100% lytic activity) and their A_{540} in the absence of a lytic agent (0% lytic activity). Separate normalization parameters were calculated at pH 5.0 and pH 7.4.

Circular dichroism studies of the lytic peptide structure

The conformational changes of GM225.1 were monitored using circular dichroism (CD) spectroscopy as the peptide becomes lytically active in the presence of lipid membranes. An Aviv 62A DS spectropolarimeter (Aviv, Lakewood, NJ) was used for the collection of CD spectra. To fully characterize this structural transition, CD spectra were obtained in the presence and absence of liposomes as a function of peptide concentration and pH. Before spectral data were collected, the sample chamber was flushed with nitrogen, and the sample cell was incubated at 37°C. Extruded liposomes (D_H = 100 nm) containing 4 μM total lipid in a 1:1 mole ratio of *N*-[2,3-(dioleyloxy)propyl]-*N,N,N*-trimethylammonium chloride (DOTMA) and 1,2-dioleoyl-3-phosphatidylethanolamine (DOPE) were then incubated with GM225.1 at 37°C for 10 min. Peptide concentrations

used for these experiments were in the range of 0.01–0.60 mg/ml (4.3–260 μM). To distinguish pH and liposome effects, GM225.1 was incubated at pH 5.0 and pH 7.4 in the presence and absence of liposomes. After incubation, the samples were scanned three times from a wavelength of 290 nm down to 195 nm. The instrument settings include a 1-nm bandwidth and a sampling time of 10 s at 1-nm intervals. Ellipticity data (θ_d, in units of degrees) were collected on a 7100/66 PowerMac with the software application CDStar b97 (Aviv). The data were then baseline corrected and converted to mean molar ellipticity per residue (θ_{mrd}), using the equation

$$\theta_{mrd} = 100^*\theta_d/(C^*I^*n_r) \quad (4)$$

where C is the molar concentration of the peptide, l is the cell pathlength, and n_r is the number of amino acid residues per peptide. The factor of 100 was used to convert molar concentration into dmole/cm^3, so that θ_{mrd} is expressed in its proper units {deg*cm^2/(dmol*residue)}. The wavelength dependence of θ_{mrd} was then used to monitor any changes in the conformation of GM225.1.

Cell transfection experiments

RAW264.7 mouse macrophages and HIG-82 rabbit synoviocytes were purchased from the American Type Culture Collection (ATCC). The C_2C_{12} mouse myoblasts were a kind gift from Dr. Robert Schwartz (Department of Cell Biology, Baylor College of Medicine). Cells were plated at an initial density near 100,000 cells/well in 20-mm tissue culture plates. Both myoblasts and macrophages were cultured in Dulbecco's modified Eagle medium (DMEM) (Gibco BRL/Life Technologies, Gaithersburg, MD) with 10% fetal bovine serum (FBS), and the HIG-82 cells were cultured in Ham's F12 medium with 10% FBS. The culture medium was changed every 48 h until the transfection experiments.

Preparation of C_2C_{12} myotubes

C_2C_{12} myoblasts were plated at a density near 100,000 cells/well in 20-mm tissue culture plates (24 wells/plate) in DMEM supplemented with 10% FBS. After reaching 100% confluency, the medium was changed to DMEM with 2% horse serum. The culture medium was then changed every 48 h for 14 days until myotube formation was complete. Before transfection, the medium was changed back to DMEM with 10% FBS. All media used for myotube preparation contained 100 units/ml penicillin and 100 μg/ml streptomycin.

Cell transfection using the peptide/DNA delivery complex

DNA concentrations were prepared in either water or 0.5 mM HEPES at volumes of 2 ml each in Fisher culture tubes at a final concentration of 33–99 μg/ml. An aliquot of carrier peptide was added to plasmids at lysine:phosphate ratios ranging from 0:1 to 6:1. The amphipathic peptide GM225.1 was added to the complex at a glutamate:DNA phosphate ratio of 1:1. The carrier peptide/plasmid/lytic peptide complexes were allowed to stand for 30 min before transfection.

One hour before transfection, the cell line was incubated in cell culture medium containing 10% FBS. Three hundred microliters of the colloidal suspension of the complex was added to each well and allowed to incubate for 5 h at 37°C. Afterward, 1 ml of the cell culture medium in 10% FBS was added to each well.

X-Gal staining for visualization of β-galactosidase activity

Cells were harvested 2 days after transfection, washed twice with PBS, and fixed for 15 min at 4°C in a solution containing 1% glutaraldehyde, 100 mM sodium phosphate buffer (PBS, pH 7.0), and 1 mM $MgCl_2$. This was followed with repeated washings in PBS and incubation at 37°C for 1 h in a staining solution containing 0.2% X-Gal, 10 mM sodium phosphate buffer (pH 7.0), 150 mM NaCl, 1 mM $MgCl_2$, 3.3 mM $K_4Fe(CN)_6{\cdot}3H_2O$, and 3.3 mM $K_3Fe(CN)_6$. After incubation, the staining solution was removed, and the cells were washed with PBS. Transfected cells were identified by their blue color with a phase-contrast microscope (Zeiss, IDO3).

Chemiluminescence assay for quantitative transfection analysis

Quantitation of the transfection efficiency was performed with the Galacto-Light chemiluminescent reporter assay kit (Tropix). Briefly, cell extracts were prepared by adding 100 μl of lysis solution containing 100 mM potassium phosphate (pH 7.8), 0.2% Triton X-100, and 1 mM dithiothreitol. Cells were then detached from the wells, transferred to a microfuge tube, and centrifuged for 10 min at 4°C to pellet any debris.

Cell extracts (5–20 μl) were mixed with 200 μl reaction buffer (100 mM sodium phosphate (pH 8.0), 1 mM magnesium chloride) and incubated at room temperature for 2 h. Samples were then mixed with 300 μl of accelerator (luminescent reagent), and β-galactosidase activity was measured as a function of luminescence with a Lumat LB 9501/16 luminometer (EG&G Berthold).

Analysis of media for the presence of human growth hormone

After transfection with the peptide/sk–human growth hormone complex, the cell culture medium for the C_2C_{12} myotubes was harvested at 24-, 48-, 72-, and 96-h time points for detection of both human growth hormone (hGH) and total protein. As a control, some myotubes were also transfected with the peptide/CMV-β-gal complex. These cells were harvested 2 days later to measure transfection efficiency with the chemiluminescence assay described above.

The hGH 100 kit (Nichols Institute Diagnostics) was used for the detection of hGH. This kit utilizes a radioimmunoassay that incorporates two monoclonal antibodies that have a high affinity for hGH. Each of the two antibodies (Ab1 and Ab2) are specific for different epitopes on the hGH protein and bind independently at their respective sites to form a sandwich complex, Ab1-hGH-Ab2. One of the antibodies is coupled to biotin (biotin Ab1), whereas the other is radiolabeled (Ab2*) with ^{125}I (courtesy of Nichols Institute Diagnostics, San Juan Capistrano, CA). Avidin beads are then added to the complex solution to form the complex (avidin bead)-(biotin Ab1)-hGH-Ab2*, which presents, after repeated washings, a radioactivity that is directly proportional to the amount of hGH. The radioactivity bound to the avidin bead was measured over a period of 1 min in a gamma counter and calibrated against a series of raidolabeled hGH standards.

Quantitation of total protein in each cell extract

Total protein from each cell extract was determined using the Coomassie Plus Protein Assay (Pierce), which measures the increase in absorbance at 595 nm that occurs when Coomassie Blue G-250 binds to protein in acidic solution. The assay was calibrated by measuring the absorbance at 595 nm of protein concentrations of bovine serum albumin (BSA) standards (Pierce) ranging from 1 to 25 μg/ml.

RESULTS

DNA condensation was observed in the presence of each of the oligolysine peptides, GM208–GM240, when the total concentration of lysine exceeded that of the DNA phosphates. PCS studies show an increased photon count rate and a reduced decay constant in the autocorrelation function, as well as a decreased hydrodynamic diameter and polydispersity index. These observations are consistent with

previous studies on condensed DNA using light scattering techniques (Bloomfield et al., 1992; Ma and Bloomfield, 1994; Post and Zimm, 1982a). Near equimolar concentrations of lysine:phosphate, there is a tendency toward aggregation, presumably due to reduced polyelectrolyte repulsion upon charge neutralization. Such effects are most noticeable at higher DNA concentrations and lower charge ratios.

A representative plot from the PCS studies is illustrated in Fig. 1, which shows the correlation between particle size and DNA concentration for a GM208/DNA complex in the presence of excess positive charge (~3/1 GM208 lysines/DNA phosphates). Fig. 1 reveals that the weighted-average hydrodynamic diameter of the complex increases with DNA concentration. Furthermore, the size distribution becomes more heterogeneous, indicating a potential limitation on the amount of DNA that can be compacted into a condensed particle. At each DNA concentration, the particle size is stable for at least 116 h.

Transmission electron micrographs confirm the particle size of the GM208/DNA complexes that were characterized by photon correlation spectroscopy. Fig. 2 *A* shows sample transmission electron micrographs of these complexes, which have a size range of 30–80 nm (outer diameter) at a plasmid concentration of 20 μg/ml and a charge ratio of three lysines per DNA phosphate. Their hydrodynamic diameter, measured by photon correlation spectroscopy, is ~30–60 nm. The majority of the GM208/DNA complexes have a toroidal morphology, whereas a proportionately smaller number of rods and spheres are also observed. This is consistent with observations of DNA condensation in the presence of polyamines (Chattoraj et al., 1978; Gosule and Schellman, 1976; Wilson and Bloomfield, 1979), poly-L-lysine (Wagner et al., 1991), and other macromolecules (Ghirlando et al., 1992; Laemmli, 1975). Upon incorporation of GM225.1, the peptide/DNA complexes are mostly spherical and are ~0–50% larger than their GM208/DNA counterparts (see Fig. 2 *B*).

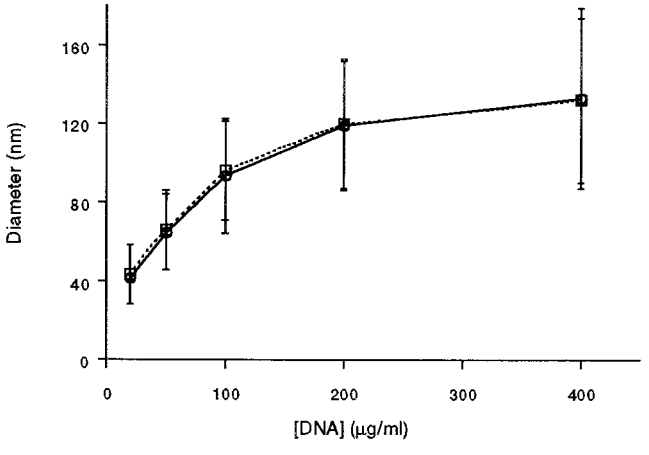

FIGURE 1 Particle sizing data of GM208/DNA complexes as a function of DNA concentration and time. ○, Time measurement taken at 0 h; □, time measurement taken at 116 h.

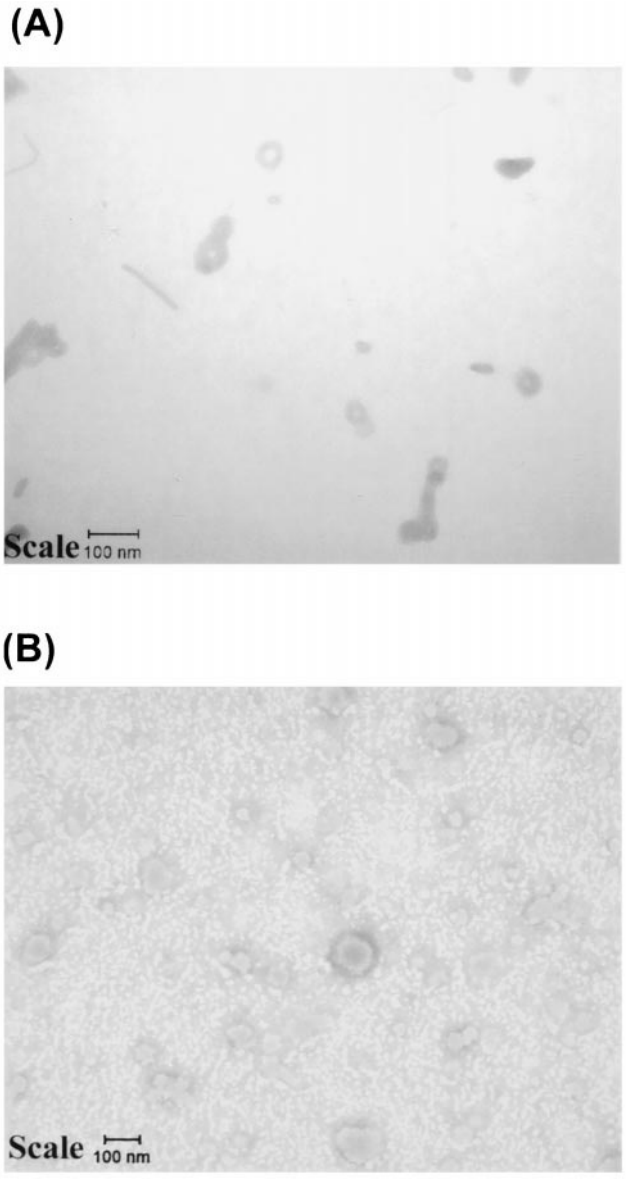

FIGURE 2 Peptide/plasmid particles observed by TEM. (*A*) Plasmid/GM208 particles prepared at a 1/3 charge ratio (−/+) and a plasmid concentration of 20 μg/ml. Original magnification, 70,000×. (*B*) Plasmid/GM208/GM225.1 particles prepared at a 1/3/1 charge ratio (−/+/−) and a concentration of 20 μg/ml DNA. Original magnification, 50,000×.

Results from the hemolysis assay (see Fig. 3) show that at concentrations between 3.5 and 104 μg/ml, the lytic activity of GM225.1 is comparable to Triton X-100 after a 1-hour incubation period at pH 5.0. Lytic activity at pH 7.4 is near zero at all peptide concentrations, except near 566 μg/ml, which is still ~18% relative to Triton X-100. A pH-dependent profile of the number of lysed RBCs (see Fig. 4) shows that the lytic activity of GM225.1 decreases dramatically when the pH is raised from 5 to 5.5, and is near zero at pH $>$ 6.0.

Fig. 5 shows representative plots from pH-dependent CD studies on GM225.1 in the presence (Fig. 5, *A* and *B*) and absence (Fig. 5 *C*) of preformed liposomes. These results

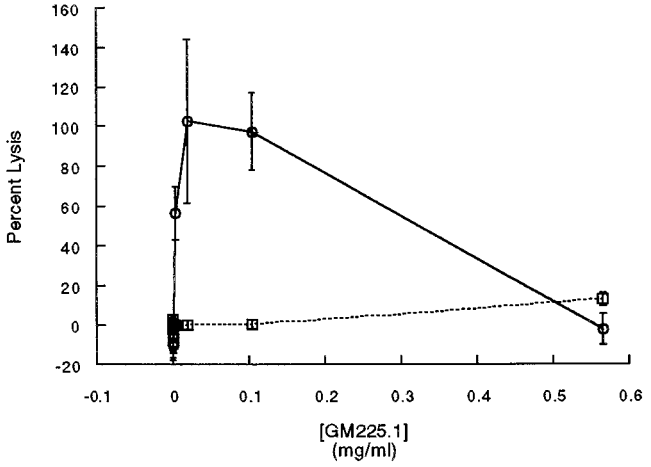

FIGURE 3 Hemolytic activity of the endoplasmic peptide. —○—, GM225.1, as a function of concentration at pH 5.0; ···□···, 7.4. Incubation time, 1 h at 37°C. From Rolland (1996).

indicate that GM225.1 undergoes a significant conformational transition in the presence of the liposomes as the pH is lowered from 7.4 to 5.0. This transition results in a significant change in molar ellipiticity at 210 nm, which is indicative of a loss in the α-helicity of the endosomolytic peptide. The conformational transition was observed at a GM225.1 concentration of 0.10 and 0.17 mg/ml, but not at 0.60 mg/ml (Fig. 5 *B*). In addition, a comparison of Fig. 5, *A* and *C*, illustrates that the liposomes are required to induce the conformational change.

The effects of a peptide-based gene delivery system on the transfection of CMV–β-Gal into 14-day C_2C_{12} myotubes are shown in Fig. 6. Transfection efficiency, as measured in terms of relative light units (RLU) per microgram of protein, is dramatically enhanced by both carrier and amphipathic peptides, relative to either peptide or plasmid alone. A visualization of the 14-day C_2C_{12} myotubes, after

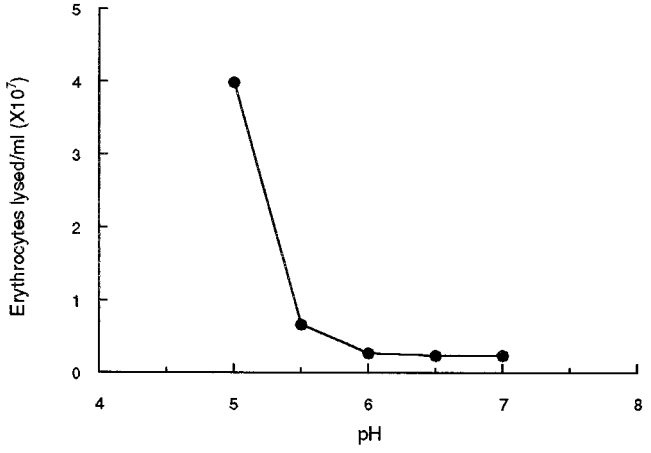

FIGURE 4 Red blood cell membrane lysis by the endoplasmic peptide GM225.1 as a function of concentration at pH. Reaction conditions include 25 μl peptide at 1 μg/μl added to 75 μl red blood cells. Incubation time, 1 h at 37°C.

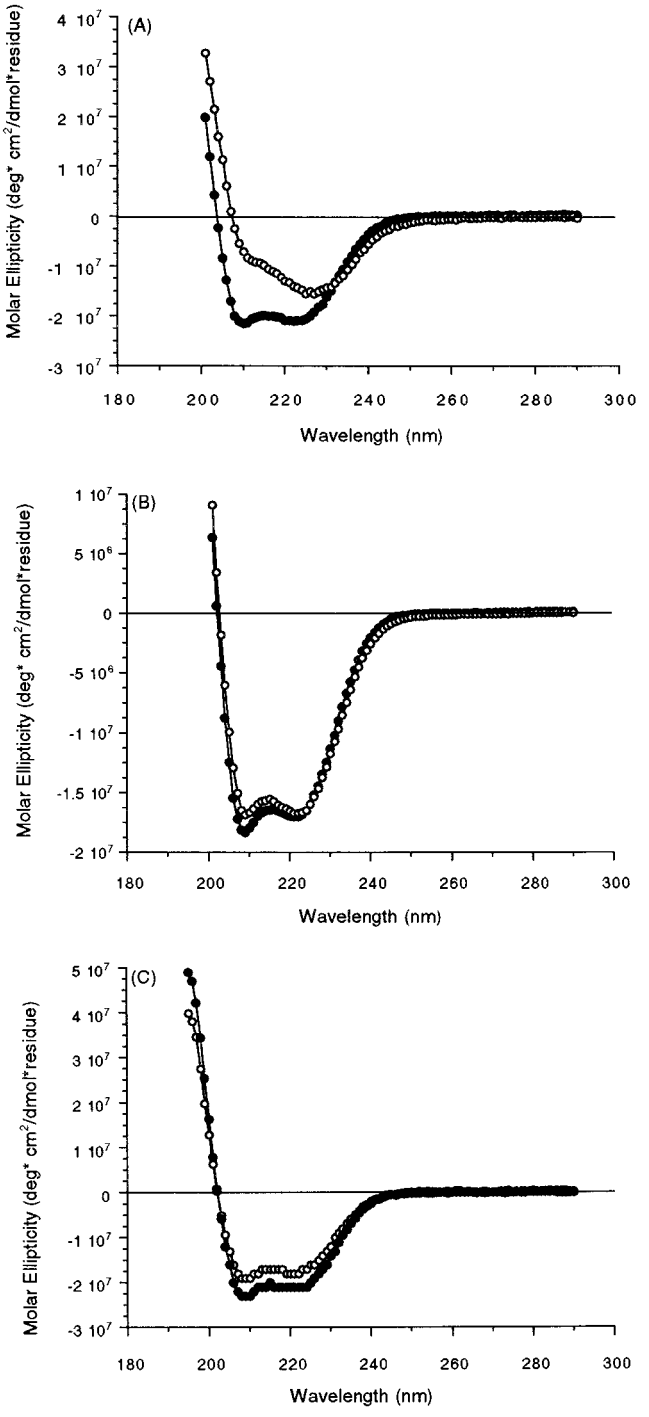

FIGURE 5 CD spectra of the endosomolytic peptide GM225.1 in the presence and absence of liposomes. Samples were incubated for 10 min at 37°C before spectral measurements. ○, pH 5.0; ●, pH 7.4. (*A*) 43 μM (0.10 mg/ml) GM225.1 plus 4 μM DOTMA:DOPE (1:1 mole ratio). (*B*) 261 μM (0.60 mg/ml) GM225.1 plus 4 μM DOTMA:DOPE (1:1 mole ratio). (*C*) 43 μM (0.10 mg/ml) GM225.1.

transfection with the peptide/plasmid complex, is illustrated in Fig. 7. β-Galactosidase activity, which is proportional to the number and intensity of blue cells, permeates the cultured myotubes and is dipersed along the tubule striations.

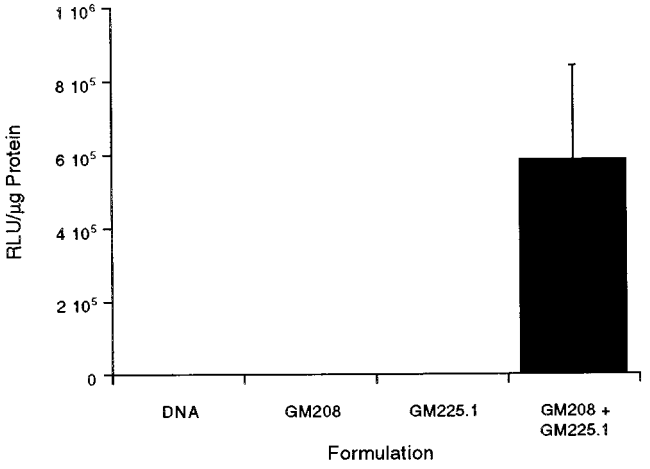

FIGURE 6 In vitro transfection of 14-day C_2C_{12} myotubes: DNA, 20 μg plasmid/well; GM208, plasmid/GM208, 1/3 (−/+) charge ratio, 20 μg plasmid/well; GM225.1, plasmid/GM225.1, 1/1 (−/−) charge ratio, 20 μg plasmid/well; GM208 + GM225.1, plasmid/GM208/GM225.1, 1/3/1 (−/+/−) charge ratio, 20 μg plasmid/well.

No such activity is observed in the absence of either the carrier or amphipathic peptide.

To better understand the relationship between the physical properties of the complexes and their ability to affect transfection efficiency in vitro, we have performed a study that compares the particle size, plasmid dose, peptide/plasmid charge ratios, and zeta potential of the complex in suspension with transfection efficiency. An examination of physical and transfection data in Table 1 reveals that transfection efficiency in C_2C_{12} myotubes increases with plasmid dose and positive zeta potential. In addition, Fig. 6 indicates that transfection efficiency is greatly enhanced by the presence of both endosomolytic and carrier peptides, the latter of which maintain colloidal stability of the particle. Thus, in the presence of endosomolytic and carrier peptides, transfection efficiency is influenced by two parameters, which can be combined into a physical index factor (I), defined by the equation

$$I = m^*_{\mathrm{DNA}}\zeta \tag{5}$$

where m_{DNA} and ζ are the plasmid dose and zeta potential, respectively. These results suggest that in addition to an adequate carrier and amphipathic agent, a sufficient amount of plasmid and high cell surface affinity are necessary for an effective gene delivery system.

To validate the use of Eq. 5 as a predictor of transfection, correlation plots were constructed between the physical index factor and the observed in vitro transfection efficiency, as exemplified in Fig. 8. This plot reveals a correlation coefficient of 0.96 between the physical index factor and transfection efficiency. Similar correlation plots were made in five separate studies utilizing three separate cell lines, the results of which are shown in Table 2. The correlation coefficients between the physical index factor and transfection efficiency range from 0.81 to 0.98.

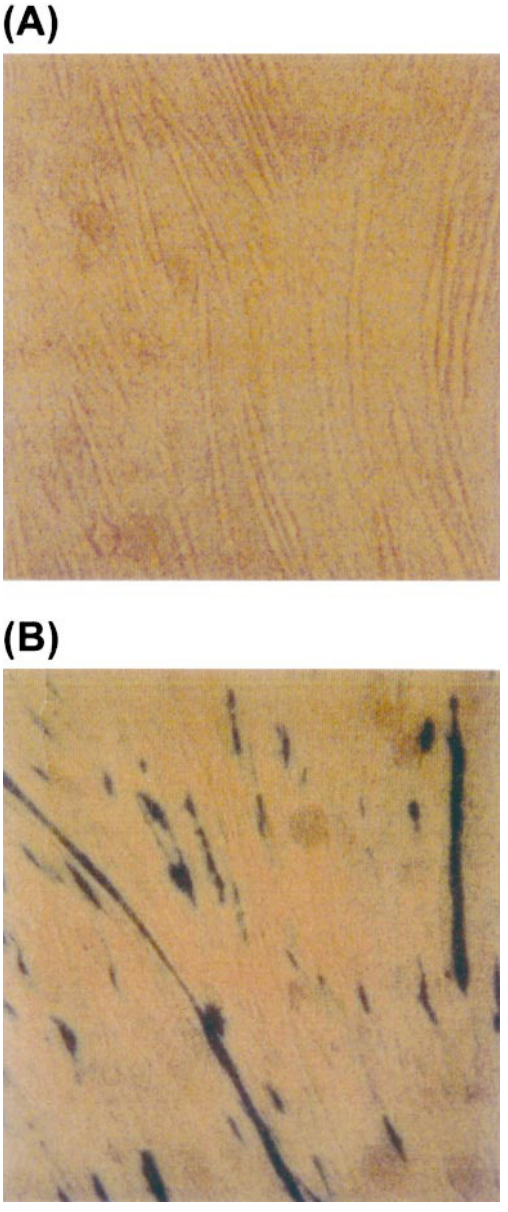

FIGURE 7 X-Gal staining of 14-day C_2C_{12} myotubes after transfection with the peptide-based gene delivery complex containing CMV-β-gal. (*A*) Cells with background β-galactosidase activity. (*B*) Cells transfected with plasmid/GM208/GM225.1, 1/3/1 charge ratio, 20 μg plasmid/well. Positive cells for β-galactosidase activity are stained dark blue.

To better understand how different peptides can influence gene delivery, we investigated the effects of the number of lysine residues in the carrier peptide on transfection efficiency. Fig. 9 *A* shows the results of transfections in C_2C_{12} myotubes using carrier peptides GM204-GM208, GM212, and GM240, corresponding to 4−8, 10, 12, and 40 core lysine residues, respectively. Maximum transfection occurs for complexes prepared with GM206-GM208, whereas transfection is attenuated when complexes are prepared with GM204-GM205 and GM240. Enhanced transfection efficiency is seen with GM205 as compared to GM204 at higher carrier peptide/plasmid ratios, although at much

TABLE 1 Transfection and physical characterization table for the peptide-based gene delivery system

Sample	Plasmid/GM208/GM225.1 (−/+/−)	DNA dose per well (μg)	ζ (mV)	D_H (nm)	RLU/μg Protein	Physical index factor (I)
1	1/0/1	10	−42	N/A	0	0
2	1/0/1	20	−62	N/A	0	0
3	1/0/1	30	−70	N/A	0	0
4	1/3/0	10	30	153	7339	0
5	1/3/0	20	29	133	15594	0
6	1/3/0	30	33	148	26600	0
7	1/6/0	10	35	127	1763	0
8	1/6/0	20	42	150	15565	0
9	1/6/0	30	67	156	0	0
10	1/3/1	10	35	187	78002	350
11	1/3/1	20	41	169	219956	820
12	1/3/1	30	39	173	309946	1170
13	1/3/1	10	41	167	39895	410
14	1/3/1	20	40	189	181314	800
15	1/3/1	30	40	202	273326	1200
16	1/6/1	10	40	142	151580	400
17	1/6/1	20	41	172	290068	820
18	1/6/1	30	41	172	386163	1230
19	1/6/1	10	40	153	125785	400
20	1/6/1	20	35	242	299749	700
21	1/6/1	30	36	222	361850	1080
22	Control*	N/A	N/A	N/A	197	N/A

*Untransfected cells.

lower levels than GM206-GM208. Thus, among the lower-molecular-weight carrier peptides, enhanced transfection efficiency is observed with each additional lysine residue. Similarly, an inspection of the sizing data in Fig. 9 *B* reveals that each additional lysine residue enhances particle stability of the formulated complex, as measured by a reduction in polydispersity and hydrodynamic diameter. The relationship between transfection efficiency and enhanced particle stability ($S_{carrier}$) created by additional lysine residues can be modeled by the expression

$$S_{carrier} = 1/(1 + k_1\exp(k_2 n)) \quad (6)$$

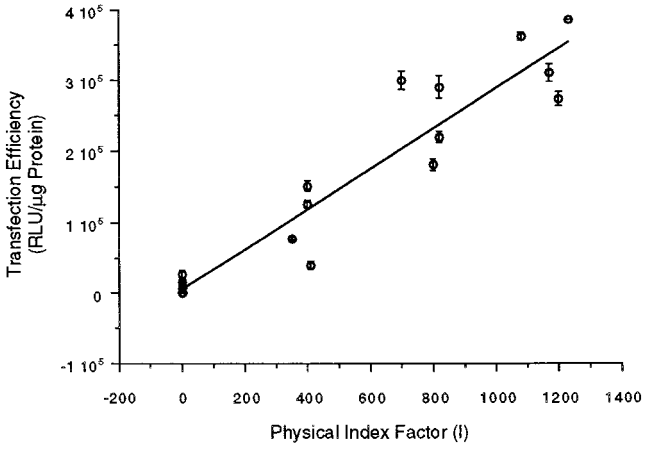

FIGURE 8 Correlation analysis between the physical index factor ($I = m_{DNA}*\zeta$) and the transfection efficiency (RLU/μg protein) in C_2C_{12} myotubes.

where k_1 is the minimum number of lysine residues required to enhance transfection efficiency via particle stabilization, k_2 is the enhanced transfection efficiency created by each additional lysine residue, and n is the number of lysine residues in the carrier peptide. This equation, which is normalized relative to maximum transfection efficiency, puts a constraint on the minimum number of lysine residues required for maximum transfection efficiency.

Fig. 9 *A* also shows that increasing the number of lysine residues on the carrier peptide can reduce transfection efficiency once this number goes beyond a certain limit. Cell toxicity, as indicated by observed cell death, suppressed protein levels, and reduced cellular metabolism, occurs in C_2C_{12} myotubes after they are transfected with a peptide/plasmid complex that contains GM240. When compared with other carrier peptides, GM240 typically reduces cellular protein production by a factor of 2–4. Similar effects of cytotoxicity have been observed when polylysine, the chain length of which is greater than 20 residues, was added to T24 cells (Deshpande, 1996), or when a 100-mer of polylysine was used to transfect HepG2 cells (L. C. Smith et al., unpublished data). The relationship between transfection

TABLE 2 Correlation between the physical index factor (I) and the transfection efficiency of peptide-based gene delivery systems

Cell line	Cell type	Correlation coefficient
C_2C_{12}	14-day mouse myotubes	0.93–0.96
HIG82	Rabbit fibroblasts	0.98
RAW264	Mouse macrophage	0.81–0.90

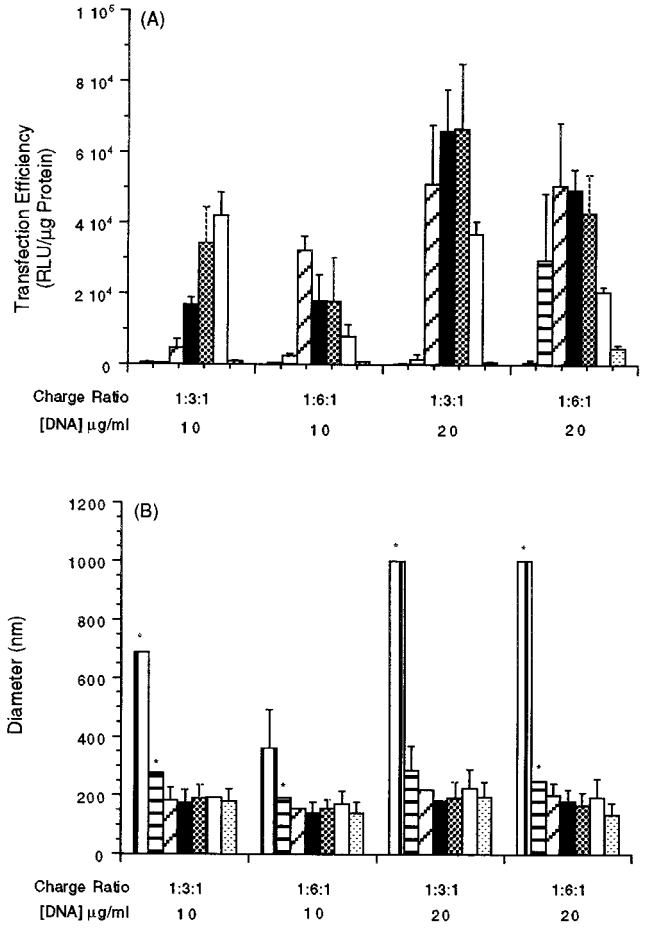

FIGURE 9 A comparison of the mean diameter of plasmid/peptide particles and transfection efficiency in C_2C_{12} myotubes as a function of the number of lysine residues in the carrier peptide. (*A*) Transfection data. (*B*) Particle sizing data. From left to right: *vertical stripes*, GM204; *horizontal stripes*, GM205; *angled stripes*, GM206; *solid black*, GM207; *Cross-hatching*, GM208; *solid white*, GM212; *dotted*, GM240. * indicates broad size distribution.

efficiency and cell toxicity (T_{carrier}) induced by additional lysine residues can be described by the inverted sigmoid function

$$T_{\text{carrier}} = 1 - 1/(1 + k_3\exp(k_4 n)) \tag{7}$$

where k_3 is the minimum number of lysine residues required to reduce transfection efficiency via cell toxicity, k_4 is the diminished transfection efficiency created by each additional lysine residue, and n is the number of lysine residues in the carrier peptide. Equation 7, which is also normalized relative to maximum transfection efficiency, places an upper limit on the number of lysine residues that can be incorporated into the carrier peptide.

To predict the optimal number of core lysines, the effects of particle stabilization and cell toxicity on transfection efficiency have been modeled as a linear combination of Eqs. 6 and 7, to yield the expression

$$S^*_{\text{carrier}}T_{\text{carrier}} = k_3\exp(-k_4 n)/[\{1 + k_1\exp(-k_2 n)\} \cdot \{1 + k_3\exp(-k_4 n)\}] \tag{8}$$

which ensures upper and lower boundary limits on the size of the carrier peptide and guarantees an optimal number of core lysines for maximum transfection. The predicted transfection efficiency from this model is shown in Fig. 10. A correlation analysis between the predicted transfection efficiency in Fig. 10 and the observed transfection efficiency (Fig. 9 *A*) as a function of the number of core lysine residues in the carrier peptide is shown in Fig. 11. This result suggests that for these peptides, the number of lysine residues on the carrier peptide influences transfection efficiency through at least two factors: instability of the DNA-peptide complex for a small number of lysine residues and cytoxicity generated by a large number of lysine residues.

The effect of utilizing a peptide-based gene delivery system in transferring the hGH gene to 14-day C_2C_{12} myotubes is illustrated in Fig. 12. This result shows an increased daily production of hGH to 22 ng/ml after 96 h if the medium is replaced every 24 h. It is also observed that hGH production reaches a maximum for a dose of 20 μg DNA/well. This observation is in contrast to β-galactosidase expression, which increases continuously to the highest dose of DNA added to the well. One hypothesis is that there may be a feedback inhibition mechanism created as a result of expression of the hGH gene. Another possibility is that the limitations of expression may be a function of the different control elements associated with the two constructs. In either case, this observation implies that Eq. 5 may require an upper limit constraint on the DNA dose. A similar possibility exists for an upper limit on zeta potential in effecting transfection efficiency.

DISCUSSION

A peptide-based gene delivery system has been shown to require both carrier and amphipathic peptides for effective in vitro cell transfection. The former provides lysine-medi-

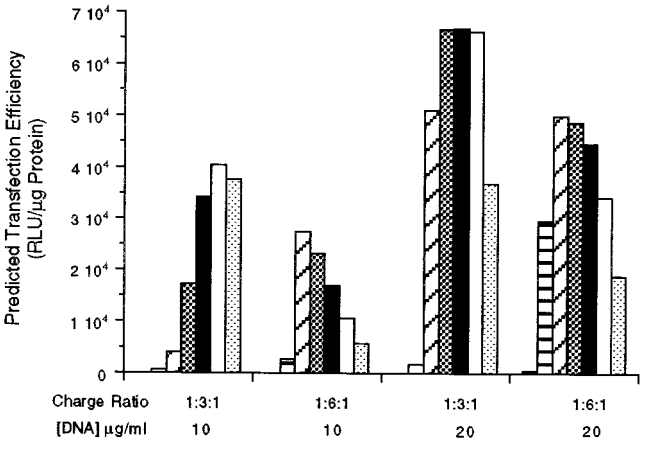

FIGURE 10 Predicted transfection efficiency in C_2C_{12} myotubes as a function of the number of lysine residues in the carrier peptide, as defined in Eq. 8. From left to right: *vertical stripes*, GM204; *horizontal stripes*, GM205; *angled stripes*, GM206; *solid black*, GM207; *cross-hatching*, GM208; *dotted*, GM240.

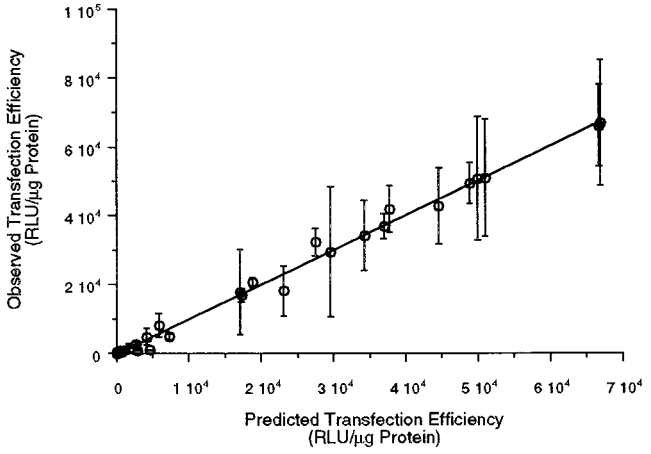

FIGURE 11 Correlation analysis between the observed transfection efficiency (Fig. 9 *A*) and that predicted by Eq. 8 (Fig. 10). The standard deviation is shown for the transfection experiment ($n = 3$).

ated charge neutralization of the DNA phosphate residues, which leads to plasmid condensation and stabilization of the resulting complex. This complex forms small particles ($D_H < 150$ nm) at DNA concentrations as high as 400 μg/ml, which are stable in water over a period of several days. Complex stability and transfection efficiency also depend on the number of lysine residues present in the carrier peptide, which must be greater than four, as suggested by particle size measurements and transfection studies in C_2C_{12} myotubes.

Previous studies (Bloomfield et al., 1980; Wilson and Bloomfield, 1979) have indicated that effective condensation requires a condensing agent with a net charge that is only greater than 2 (in one instance, it has been shown that a complex involving the transition metal Mn^{2+} is also an effective condensing agent; Ma and Bloomfield, 1994). These studies were performed at low DNA concentrations

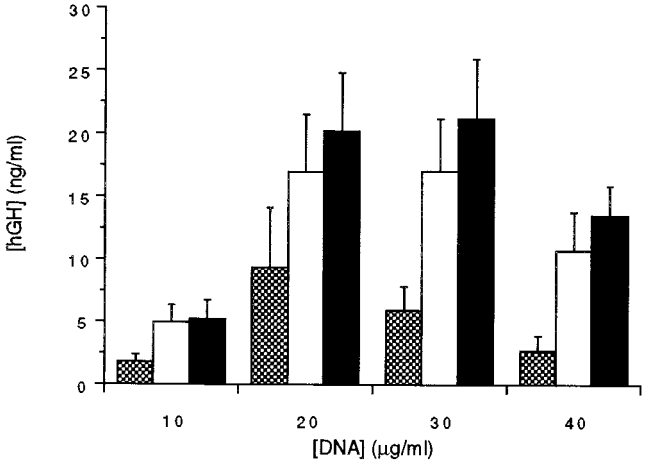

FIGURE 12 Production of human growth hormone (hGH) as a function of DNA dose and media replacement every 24 h after transfection with plasmid/GM208/GM225.1 complexes (1/3/1 −/+/−). *Gray column*, media replacement at 48 h; *white column*, 72 h; *black column*, 96 h.

(<20 μg/ml), and we observe similar results under similar conditions. However, we observe an increase in particle size and polydispersity at higher DNA concentrations. This implies that the condensate may become increasingly unstable. Normally, we perform transfection studies at DNA concentration ranges from 33 to 100 μg/ml. At these concentrations, a greater number of charged residues per carrier peptide may be required to maintain particle stability.

As an alternative explanation, the higher charge requirement on the carrier peptide may be necessary at higher plasmid concentrations to maintain the gene delivery complex in its activated state. Previous studies (Arscott et al., 1995) have shown that different complex morphologies can be obtained when the DNA concentration is raised. The unique morphologies formed at elevated plasmid concentrations can lead to complexes that have lower transfection activities. A more highly charged peptide can provide a barrier to the formation of these different structural states and maintain transfection integrity. These hypotheses are consistent with Fig. 9, which shows that a reduction in particle size occurs simultaneously with enhanced transfection efficiency when the number of lysine residues on the carrier peptide is greater than four.

GM225.1, which was designed to induce a pH-dependent lytic effect on biological membranes, is expected to be required in the peptide/plasmid complex for endosomal release after particle uptake via endocytosis. Evidence for an endosomolytic effect of GM225.1 can be observed not only by the in vitro transfection assays performed in this study, but also by the results of the hemolytic assays that demonstrate a pH-dependent lysis of red blood cell membranes. One interesting observation from the hemolytic assays is that when the concentration of GM225.1 is increased, the lytic activity increases sharply at low concentrations, reaches a maximum, and then decreases to almost zero. One explanation of this observation is that the increase in the concentration of GM225.1 eventually leads to aggregate formation that inactivates this peptide. GM225.1 tends to aggregate readily, and the presence of 6 M guanidine HCl is required to prevent the formation of multimeric peptide structures (J. T. Sparrow and L. C. Smith, unpublished data).

The structural properties of GM225.1 are comparable to those of other lytic peptides derived from the influenza virus hemagglutinin (HA) (Doms et al., 1991; Ojcius and Young, 1991; Plank et al., 1994; Ramalho-Santos et al., 1993; Wagner et al., 1992; Wharton et al., 1988) and the GALA peptide (Parente et al., 1990a,b; Subbarao et al., 1987). Such properties include an α-helical structure, as evidenced by circular dichroism, and the N-terminal hydrophobic GLF motif that is considered to enhance membrane insertion (Doms et al., 1991; Ojcius and Young, 1991; Plank et al., 1994; Ramalho-Santos et al., 1993; Wagner et al., 1992). Interestingly, our CD studies reveal that the α-helical structure of GM225.1 is significantly reduced at lower peptide concentrations, in the presence of cationic liposomes, and at a lowered pH of 5.0. These conditions are consistent with

those associated with increased hemolytic activity, which suggests that the observed structural transition leads to an activated state of GM225.1. Although this transition is most pronounced in the presence of cationic liposomes, similar perturbations of the CD spectra can be observed at pH 5.0, when low concentrations of GM225.1 (<0.1 mg/ml) are incubated with anionic liposomes.

Finally, GM225.1 is designed with distinct hydrophobic/hydrophilic faces in which the latter subtends an angle greater than 120°, which has been suggested to be required for membrane insertion (Tytler et al., 1993). This is most aptly illustrated in a helical wheel diagram of GM225.1, which shows the hydrophobic and hydrophilic portions of the peptide chain (Fig. 13).

We have correlated several physical properties of the complex with in vitro transfection efficiency. There is a linear correlation between combinations of zeta potential, DNA dose, the presence of carrier and lytic peptides, and transfection efficiency. These observations have been made in different cell lines, including macrophages, synoviocytes, and myotubes. The physical index factor (I), which provides a mathematical description of the physical properties required for transfection, illustrates a need for an effective DNA dose and a requirement for cell surface affinity (as measured by the ζ potential). The incorporation of the ζ potential into the physical index factor is essential for the prediction of in vitro transfection efficiency, because it provides a real measure of the affinity of the gene delivery complex for charged cell surfaces. One may argue that the concentration of carrier peptide in solution may serve as a substitute for the ζ potential in predicting affinity between the cell surface and the gene delivery complex. However, we find experimentally that the solution concentration of carrier peptide is inadequate in predicting transfection efficiency. This occurs because the number of carrier peptides incorporated into the gene delivery complex is influenced by factors other than the solution concentration of carrier peptide. Such factors include counterion saturation of the DNA phosphates, misalignment of the charge spacings between the carrier peptide and plasmid DNA, and sequestration of the carrier peptide by the endosomolytic peptide. Because the number of peptides incorporated into the plasmid can be influenced by several different factors, the zeta potential is a better indicator of transfection efficiency, because it absorbs all of these factors into one experimentally measurable parameter.

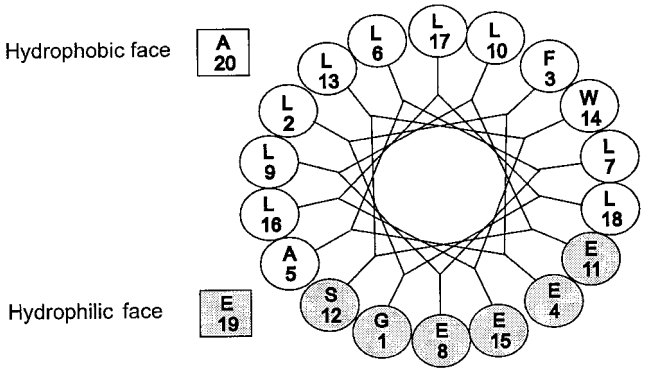

FIGURE 13 Helical wheel of the endosomolytic peptide, GM225.1. *White circles and square*, hydrophobic face; *light gray circles and square*, hydrophilic face.

The requirement of a carrier peptide in the complex can be defined more specifically as a requirement for a carrier peptide with a specific number of lysine residues. Although we have not ruled out other factors, such as excessive complex stability, our experimental evidence suggests that the ideal number of lysine residues depends upon optimization between complex stability and minimum cell toxicity. The requirement of a carrier peptide with a specific number of lysine residues places an additional constraint on the physical properties necessary for an effective peptide-based gene delivery system. When this constraint, as defined in Eq. 8, is incorporated into Eq. 5, the following relationship is obtained:

$$I = S^*_{\text{carrier}} T^*_{\text{carrier}} m^*_{\text{DNA}} \zeta \tag{9}$$

which may be expanded to yield the expression

$$I = k_3 \exp(-k_4 n)/[\{1 + k_1 \exp(-k_2 n)\} \cdot \{1 + k_3 \exp(-k_4 n)\}]^* m^*_{\text{DNA}} \zeta \tag{10}$$

The results from Eq. 10 are still by no means complete. However, it does provide an initial understanding between the physical properties of the particle and transfection efficiency.

To qualify the use of the peptide/plasmid complex as a therapeutic gene delivery system, we have shown its capacity to deliver the therapeutic human growth hormone gene to 14-day C_2C_{12} myotubes. The successful delivery of this gene to well-differentiated muscle cells and the prolonged gene expression observed to increase over a 4-day period illustrate the potential usefulness of employing peptide-based delivery systems for gene therapy.

We acknowledge the following scientists at GeneMedicine for their contributions: the Process Manufacturing Group for providing plasmid, Dr. Ching-Hsuan Tung in the Gene Delivery Department for supplying peptides GM208 and GM225.1, Dr. Ross Durland for useful discussions, and Dr. Hiroaki Nitta for processing Fig. 7. We also acknowledge Prof. John Olson and Dr. Jeff Nichols (Rice University) for providing their instrumentation and valuable expertise for our circular dichroism studies.

REFERENCES

Arscott, P. G., C. Ma, J. R. Wenner, and V. A. Bloomfield. 1995. DNA condensation by cobalt hexaamine (III) in alcohol-water mixtures: dielectric constant and other solvent effects. *Biopolymers.* 36:345–364.

Barany, G., and R. B. Merrifield. 1980. Solid phase peptide synthesis. *In* The Peptides: Analysis, Synthesis, Biology. Academic Press, New York.

Bloomfield, V. A. 1992. Condensation of DNA by multivalent cations: considerations on mechanism. *Biopolymers.* 31:1471–1481.

Bloomfield, V. A. 1996. DNA condensation. *Curr. Opin. Struct. Biol.* 6:334–341.

Bloomfield, V. A., S. He, A.-Z. Li, and P. G. Arscott. 1992. Light scattering studies of DNA condensation. *In* Laser Light Scattering in Biochemistry. The Royal Society of Chemistry, Cambridge, England.

Bloomfield, V. A., R. W. Wilson, and D. C. Rau. 1980. Polyelectrolyte effects in DNA condensation by polyamines. *Biophys. Chem.* 11: 339–343.

Boussif, O., F. Lezoualc'h, M. A. Zanta, M. D. Mergny, D. Scherman, B. Demeneix, and J.-P. Behr. 1995. A versatile vector for gene and oligonucleotide transfer into cells in culture and in vivo: polyethylenimine. *Proc. Natl. Acad. Sci. USA.* 92:7297–7301.

Chattoraj, D. K., L. C. Gosule, and J. A. Schellman. 1978. DNA condensation with polyamines. II. Electron microscopic studies. *J. Mol. Biol.* 121:327–337.

Cotten, M., F. Laengle-Rouault, H. Kirlappos, E. Wagner, K. Mechtler, M. Zenke, H. Beug, and M. L. Birnstiel. 1990. Transferrin-polycation-mediated introduction of DNA into human leukemic cells: stimulation by agents that affect the survival of transfected DNA or modulate transferrin receptor levels. *Proc. Natl. Acad. Sci. USA.* 87:4033–4037.

Cotten, M., E. Wagner, and M. L. Birnstiel. 1993. Receptor mediated transport of DNA into eukaryotic cells. *Methods Enzymol.* 217: 618–644.

Deshpande, D. 1996. Inhibition of C-Ha-ras oncogene expression by antisense oligonucleotides using EGF receptor mediated delivery systems. Ph.D. thesis. Department of Pharmaceutical Sciences, University of West Virginia, Morgantown. 1–150.

Doms, R. W., J. White, F. Boulay, and A. Helenius. 1991. Influenza virus hemagglutinin and membrane fusion. *In* Membrane Fusion. Marcel Dekker, New York.

Dowty, M. E., and J. A. Wolff. 1994. Possible mechanisms of DNA uptake in skeletal muscle. *In* Gene Therapeutics: Methods and Applications of Direct Gene Transfer. Birkhäuser, Boston.

Duguid, J. G., and V. A. Bloomfield. 1996. Electrostatic effects on the stability of condensed DNA in the presence of divalent cations. *Biophys. J.* 70:2838–2846.

Eickbush, T. H., and E. N. Moudrianakis. 1978. The compaction of DNA helices into either continuous supercoils or folded-fiber rods and toroids. *Cell.* 13:295–306.

Erbacher, P., A. C. Roche, M. Monsigny, and P. Midoux. 1995. Glycosylated polylysine/DNA complexes: gene transfer efficiency in relation with the size and the sugar substition level of glycosylated polylysines and with the plasmid size. *Bioconjug. Chem.* 6:401–410.

Evdokimov, Y. M., N. M. Akimenko, N. E. Glukhova, A. S. Tikhonenko, and Y. M. Varshavskii. 1973. Production of the compact form of double-stranded DNA in solution in the presence of poly(ethylene glycol). *Mol. Biol.* 7:124–132 (transl. from Russian).

Evdokimov, Y. M., T. L. Pyatigorskaya, O. T. Polivtsev, N. M. Akimenko, D. Y. Tsvankin, and Y. M. Varshavskii. 1976. Compact form of DNA in solution. VIII. X-ray diffraction investigation of compact DNA particles formed in aqueous salt solutions containing poly(ethylene glycol). *Mol. Biol.* 10:992–999 (transl. from Russian).

Fattal, E., S. Nir, R. A. Parente, and F. C. J. Szoka. 1994. Pore-forming peptides induce rapid phospholipid flip-flop in membranes. *Biochemistry.* 33:6721–6731.

Felgner, P. S., T. R. Gladek, M. Holm, R. Roman, H. W. Chan, M. Wenz, J. P. Northrop, G. M. Ringold, and M. Danielsen. 1987. Lipofectin: a highly efficient, lipid-mediated DNA-transfection procedure. *Proc. Natl. Acad. Sci. USA.* 84:7413–7417.

Gagne, L., J. T. Conary, A. E. Canonico, K. L. Brigham, and H. Schreier. 1994. Liposome-mediated gene delivery. II. In vitro toxicity of cationic liposome DNA plasmid complexes. *Proc. Int. Symp. Control. Rel. Bioact. Mater.* 21:236–237.

Gao, X., and L. Huang. 1995. Cationic liposome-mediated gene transfer. *Gene Ther.* 2:710–722.

Gershon, H., R. Ghirlando, S. B. Guttman, and A. Minsky. 1993. Mode of formation and structural features of DNA-cationic liposome complexes used for transfection. *Biochemistry.* 32:7143–7151.

Ghirlando, R., E. J. Wachtel, T. Arad, and A. Minsky. 1992. DNA packaging induced by micellar aggregates: a novel in vitro DNA condensation system. *Biochemistry.* 31:7110–7119.

Gosule, L. C., and J. A. Schellman. 1976. Compact form of DNA induced by spermidine. *Nature.* 259:333–335.

Gottschalk, S., R. J. Cristiano, L. C. Smith, and S. L. C. Woo. 1993. Folate receptor mediated DNA delivery into tumor cells: potosomal disruption results in enhanced gene expression. *Gene Ther.* 1:185–191.

Gottschalk, S., J. T. Sparrow, J. Hauer, M. P. Mims, F. E. Leland, S. L. C. Woo, and L. C. Smith. 1996. A novel DNA/peptide complex for efficient gene transfer and expression in mammalian cells. *Gene Ther.* 3:448–457.

Gustafsson, J., G. Arvidson, G. Karlsson, and M. Almgren. 1995. Complexes between cationic liposomes and DNA visualized by cryo-TEM. *Biochim. Biophys. Acta.* 1235:305–312.

Haensler, J., and F. C. Szoka. 1993. Polyamidoamine cascade polymers mediated efficient transfection of cells in culture. *Bioconjug. Chem.* 4:372–379.

Hancock, W. S., and J. T. Sparrow. 1981. Use of mixed-mode high-performance liquid chromatography for the separation of peptide and protein mixtures. *J. Chromatogr.* 206:71–82.

Hancock, W. S., and J. T. Sparrow. 1984. HPLC Analysis of Biological Compounds. Chromatographic Science Series. Marcel Dekker, New York.

Haynes, M., R. A. Garrett, and W. B. Gratzer. 1970. Structure of nucleic acid-poly base complexes. *Biochemistry.* 9:4410–4416.

Hirschman, S. Z., M. Leng, and G. Felsenfeld. 1967. Interaction of spermine and DNA. *Biopolymers.* 5:227–233.

Hud, N. V. 1995. Double-stranded DNA organization in bacteriophage heads: an alternative toroid-based model. *Biophys. J.* 69:1355–1362.

Hud, N. V., K. H. Downing, and R. Balhorn. 1995. A constant radius of curvature model for the organization of DNA in toroidal condensates. *Proc. Natl. Acad. Sci. USA.* 92:3581–3585.

Kabanov, V. A., and V. A. Kabanov. 1995. DNA complexes with polycations for the delivery of genetic material into cells. *Bioconjug. Chem.* 6:7–20.

Labat-Moleur, F., A.-M. Steffan, C. Brisson, H. Perron, O. Feugeas, P. Furstenberger, F. Oberling, E. Brambilla, and J.-P. Behr. 1996. An electron microscopy study into the mechanism of gene transfer with lipopolyamines. *Gene Ther.* 3:1010–1017.

Laemmli, U. K. 1975. Characterization of DNA condensates induced by poly(ethylene oxide) and polylysine. *Proc. Natl. Acad. Sci. USA.* 72: 4288–4292.

Ledley, F. D. 1994. Non-viral gene therapy. *Curr. Opin. Biotechnol.* 5:626–636.

Ledley, F. D. 1995. Nonviral gene therapy: the promise of genes as pharmaceutical products. *Hum. Gene Ther.* 6:1129–1144.

Legendre, J.-Y., and F. C. Szoka. 1992. Delivery of plasmid DNA into mammalian cell lines using pH-sensitive liposomes: comparison with cationic liposomes. *Pharm. Res.* 9:1235–1242.

Legendre, J.-Y., and F. C. J. Szoka. 1993. Cyclic amphipathic peptide-DNA complexes mediated high-efficiency transfection of adherent mammalian cells. *Proc. Natl. Acad. Sci. USA.* 90:893–897.

Lerman, L. S. 1971. A transition to a compact form of DNA in polymer solutions. *Proc. Natl. Acad. Sci. USA.* 68:1886–1890.

Li, A., L. Hu, Z. Wei, V. A. Bloomfield, and P. G. Arscott. 1991. A theoretical model of multi-molecular condensation of DNA. *Acta Biophys. Sinica.* 7:455–459.

Ma, C. 1992. DNA condensation in alcohol-water mixtures. M.S. thesis. Department of Biochemistry, University of Minnesota, St. Paul. 1–88.

Ma, C., and V. A. Bloomfield. 1994. Condensation of supercoiled DNA induced by $MnCl_2$. *Biophys. J.* 67:1678–1681.

Manning, G. S. 1980. Thermodynamic stability theory for DNA doughnut shapes induced by charge neutralization. *Biopolymers.* 19:37–59.

Manning, G. S. 1981. The possibility of intrinsic local curvature in DNA toroids. *Biopolymers.* 20:1261–1270.

Manning, G. S. 1985. Packaged DNA: an elastic model. *Cell. Biophys.* 7:57–89.

Midoux, P., C. Mendes, A. Legrand, J. Raimond, R. Mayer, M. Monsigny, and A. C. Roche. 1993. Specific gene transfer mediated by lactosylated poly-L-lysine into hepatoma cells. *Nucleic Acids Res.* 21:871–878.

Monsigny, M., A.-C. Roche, P. Midoux, and R. Mayer. 1994. Glycoconjugates as carriers for specific delivery of therapeutic drugs and genes. *Adv. Drug Delivery Rev.* 14:1–24.

Ojcius, D. M., and J. D. E. Young. 1991. Cytolytic pore-forming proteins and peptides: is there a common structural motif? *Trends Biochem. Sci.* 16:225–229.

Olins, D. E., A. L. Olins, and P. H. von Hippel. 1967. Model nucleoprotein complexes: studies on the interaction of cationic homopolypeptides with DNA. *J. Mol. Biol.* 24:157–176.

Parente, R. A., L. Nadasdi, N. K. Subbarao, and F. C. Szoka, Jr. 1990a. Association of a pH-sensitive peptide with membrane vesicles: role of amino acid sequence. *Biochemistry.* 29:8713–8719.

Parente, R. A., S. Nir, and F. C. Szoka, Jr. 1990b. Mechanism of leakage of phospholipid vesicle contents induced by the peptide GALA. *Biochemistry.* 29:8720–8728.

Plank, C., K. Aztloukal, M. Cotten, K. Mechtler, and E. Wagner. 1992. Gene transfer into hepatocytes using asialoglycoprotein receptor mediated endocytosis of DNA complexed with an artificial tetra-antennary galactose ligand. *Bioconjug. Chem.* 3:533–539.

Plank, C., B. Oberhauser, K. Mechtler, C. Koch, and E. Wagner. 1994. The influence of endosome-disruptive peptides on gene transfer using synthetic virus-like gene transfer systems. *J. Biol. Chem.* 269: 12918–12924.

Post, C. B., and B. H. Zimm. 1979. Internal condensation of a single DNA molecule. *Biopolymers.* 18:1487–1501.

Post, C. B., and B. H. Zimm. 1982a. Light scattering study of DNA condensation: competition between collapse and aggregation. *Biopolymers.* 21:2139–2160.

Post, C. B., and B. H. Zimm. 1982b. Theory of DNA condensation: collapse vs. aggregation. *Biopolymers.* 21:2123–2137.

Rädler, J. O., I. Koltover, T. Salditt, and C. R. Safinya. 1997. Structure of DNA-cationic liposome complexes: DNA intercalaction in multilamellar membranes in distinct interhelical packing regimes. *Science.* 275: 810–814.

Ramalho-Santos, J., S. Nir, N. Duzgunes, A. P. de Carvalho, and M. C. P. de Lima. 1993. A common mechanism for influenza virus fusion activity and inactivation. *Biochemistry.* 32:2771–2779.

Reid, G. E., and R. J. Simpson. 1992. Automated solid-phase peptide synthesis: use of 2–1h-benzotriazol-1-yl-1133-tetramethyluronium tetrafluoroborate for coupling of *tert*-butyloxycarbonyl amino acids. *Anal. Biochem.* 200:301–309.

Reimer, D. L., Y. P. Zhang, S. Kong, J. J. Wheeler, R. W. Graham, and M. B. Bally. 1995. Formation of novel hydrophobic complexes between cationic lipids and plasmid DNA. *Biochemistry.* 34:12877–12883.

Remy, J.-S., A. Kichler, V. Mordvinov, F. Schuber, and J.-P. Behr. 1995. Targeted gene transfer into hepatoma cells with lipopolyamine-condensed DNA particles presenting galactose ligands: a stage toward artificial viruses. *Proc. Natl. Acad. Sci. USA.* 92:1744–1748.

Richards, K. E., R. C. Williams, and R. Calendar. 1973. Mode of DNA packing within bacteriophage heads. *J. Mol. Biol.* 78:255–259.

Rolland, A. 1996. Controllable gene therapy: recent advances in non-viral gene delivery. *In* Targeting of Drugs, Vol. 5, Strategies for Oligonucleotide and Gene Delivery in Therapy. Plenum Press, New York.

Rolland, A. 1998. From gene to gene medicine: recent advances in non-viral gene delivery. *In* Crit. Rev. Ther. Drug Carrier Syst., vol. 15. S. D. Bruck, editor. Begell House, New York.

Rolland, A. P., and E. Tomlinson. 1996. Controllable gene therapy using nanoparticle systems. *In* Artificial Self-Assembling Systems for Gene Delivery. American Chemical Society, Washington, DC.

Shapiro, J. T., M. Leng, and G. Felsenfeld. 1969. Deoxyribonucleic acid-polylysine complexes. Structure and nucleotide specificity. *Biochemistry.* 8:3219–3231.

Smith, J. G., R. L. Walzem, and J. B. German. 1993. Liposomes as agents of DNA transfer. *Biochim. Biophys. Acta.* 1154:327–340.

Sternberg, B., F. L. Sorgi, and L. Huang. 1994. New structures in complex formation between DNA and cationic liposomes visualized by freeze-fracture electron microscopy. *FEBS Lett.* 356:361–366.

Subbarao, N. K., R. A. Parente, F. C. Szoka, Jr., L. Nadasdi, and K. Pongracz. 1987. pH-dependent bilayer destabilization by an amphipathic peptide. *Biochemsitry.* 26:2964–2972.

Tang, M. X., and F. C. J. Szoka. 1997. Biophysical and colloidal aspects of DNA compaction. *In* Self-Assembling Complexes for Gene Delivery: From Chemistry to Clinical Trial. John Wiley and Sons, New York.

Tomlinson, E., and A. P. Rolland. 1996. Pharmaceutics of non-viral gene delivery systems. *J. Controlled Release.* 39:357–372.

Trubetskoy, V. S., V. P. Torchilin, S. Kennel, and L. Huang. 1992. Cationic liposomes enhance targeted delivery and expression of exogenous DNA mediated by N-terminal modified poly(L-lysine)-antibody conjugate in mouse lung endothelial cells. *Biochim. Biophys. Acta.* 1131:311–313.

Tytler, E. M., J. P. Segrest, R. M. Epand, S. Q. Nie, R. F. Epand, V. K. Mishra, Y. V. Venkatachalapathi, and G. M. Anantharamaiah. 1993. Reciprocal effects of apolipoprotein and lytic peptide analogs on membranes. *J. Biol. Chem.* 268:22112–22118.

Wagner, E., M. Cotten, R. Foisner, and M. L. Birnstiel. 1991. Transferrin-polycation-DNA complexes: the effect of polycations on the structure of the complex and DNA delivery to cells. *Proc. Natl. Acad. Sci. USA.* 88:4255–4259.

Wagner, E., C. Plank, K. Zatloukal, M. Cotten, and M. L. Birnstiel. 1992. Influenza virus hemagglutinin HA-2 N-terminal fusogenic peptides augment gene transfer by transferrin-polylysine/DNA complex: towards a synthetic virus-like gene transfer vehicle. *Proc. Natl. Acad. Sci. USA.* 89:7934–7938.

Wagner, E., M. Zenke, M. Cotten, H. Beug, and M. L. Birnstiel. 1990. Transferrin-polycation conjugates as carriers for DNA uptake into cells. *Proc. Natl. Acad. Sci. USA.* 87:3410–3414.

Wang, C.-Y., and L. Huang. 1989. High efficient DNA delivery mediated by pH-sensitive Immunoliposomes. *Biochemistry.* 28:9508–9514.

Wharton, S. A., S. R. Martin, R. W. H. Ruigrok, J. J. Skehel, and D. C. Wiley. 1988. Membrane fusion by peptide analogues of influenza virus haemagglutinin. *J. Gen. Virol.* 69:1847–1857.

Widom, J., and R. L. Baldwin. 1980. Cation-induced toroidal condensation of DNA: studies with $Co^{3+}(NH_3)_6$. *J. Mol. Biol.* 144:431–453.

Widom, J., and R. L. Baldwin. 1983. Monomolecular condensation of λ-DNA induced by cobalt hexammine. *Biopolymers.* 22:1595–1620.

Wilson, R. W., and V. A. Bloomfield. 1979. Counterion-induced condensation of deoxyribonucleic acid. A light-scattering study. *Biochemistry.* 18:2192–2196.

Wu, G. Y., and C. H. Wu. 1987. Receptor mediated in vitro gene transformation by a soluble DNA carrier system. *J. Biol. Chem.* 262: 4429–4432.

Wu, G., and C. Wu. 1988a. Evidence for targeted gene delivery to HepG2 hepatoma cells in vitro. *Biochemistry.* 27:887–892.

Wu, G. Y., and C. H. Wu. 1988b. Receptor-mediated gene delivery and expression in vivo. *J. Biol. Chem.* 263:14621–14624.

Zhou, X., A. Klibanov, and L. Huang. 1991. Lipophilic polylysines mediate efficient DNA transfection in mammalian cells. *Biochim. Biophys. Acta.* 1065:8–14.